



Propagation and Optimisation

Assignment II

Lorenz Veithen

Lunar Ascent Trajectory Propagation and Optimisation

Acceleration and Environment Models Selection

Lecturers: Dr. D. Dirkx
Github repository link: https://github.com/LorenzVeithen/PropagationOptimisation_Lorenz_Veithen
May 31, 2023

Hours spent: \approx 45h

Lorenz Veithen 5075211

Cooperating Students: Srujan Vaidya (5072034) and Oliver Ross (5008042)



¹Cover Image URL: <https://www.bbc.com/news/science-environment-50322402>

1 Propagation Requirements

In the previous assignment, a series of requirements on the benchmark, numerical and physical models, as well as CPU time, were given. Numerical, physical and CPU time requirements are re-iterated upon in Table 1. For a justification of PROP-1,2,3, refer to Veithen [1] (section 1). As the aim of this work is to optimise the trajectory, PROP-4 was reduced from 2s to 0.5s based on the integrator-propagator combination capabilities seen in [1]. This will permit to perform 4x more propagations, and hence survey a larger part of the design space. Furthermore, in [1], a variable step RKF4(5) integrator with a Cowell propagator was selected. With absolute and relative tolerances smaller than $1e-7$, maximum position and velocity numerical errors of $5.26e-2m$ and $6.95e-05m/s$ respectively are guaranteed¹. However, a maximum step size of 20s was set in this work to ensure a denser output towards the end of the propagation (necessary as 5 points are removed on either boundaries after the interpolation due to Runge's phenomenon). This is assumed to have no impact on the accuracy analysis of the models, as the integrator accuracy is two orders of magnitude smaller than PROP-1,2,3. However, this will result in longer CPU run time than will be used in the optimisation.

Table 1: Propagation requirements. Note that only PROP-4 was adjusted

REQ ID	Requirement
PROP-1	The position accuracy of the physical modelling shall be 10m or smaller.
PROP-2	The velocity accuracy of the physical modelling shall be 0.1m/s or smaller.
PROP-3	The physical mass modelling accuracy shall be 0.01kg or smaller.
PROP-4	CPU time per run shall be 0.5s or smaller.

2 Acceleration en Environment Models

2.1 Settings Selection

For a lunar ascent trajectory, the major accelerations are the engine thrust and Moon gravity field. Moreover, as the trajectory is propagated from altitudes ranging from 100m to 100km altitude, spherical harmonics (SH) of the gravity field will have a significant effect on the propagation. According to Boere [2] and Roncoli [3] a minimum 50x50 degree and order (D/O) field is necessary for lunar missions in the altitude range 30-100km, and even higher D/O are required in the 0.1-30km range. However, for optimisation purposes, it is more important to be able to propagate the trajectory a high number of times to better survey the design space, than have a very accurate propagation. Therefore, the majority of literature on the optimisation of lunar ascent/descent trajectories simplifies the acceleration environment to a point mass gravity field of the Moon, or only take D/O up to (2,2) only [4, 5]. Additionally, the trajectory starts very close to the ground, inside the circumscribing sphere of the Moon, which can cause the SH gravity field to diverge (this will be analysed below). For the selection of the acceleration model, the following will be considered:

- **Earth:** point-mass (PM) is a 1st order perturbation [2], and its proximity means that its orientation (SH) can be relevant.
- **Sun PM:** this perturbation is the second-largest perturbation for lunar descent trajectories according to Boere [2].
- **Solar system planets² PM:** are considered, although they are not expected to have a major effect on the trajectory due to the short duration of the mission ($\sim 450s$), the large distance, and small mass (compared to the Sun).
- The **relativistic corrections** (Lens Stirling, de Sitter with the Sun as central body, and Schwarzschild) and **cannonball radiation pressure** are considered despite being expected to be negligibly small due to the short mission duration.

Following, a variety of environment models are investigated with the aim to reduce the propagation's computational load.

- **Atmosphere:** the Moon's atmosphere is very tenuous and will not be considered in this work [2].
- **Gravity field variations:** the largest variations in the Moon SH coefficients are five orders of magnitude smaller than their mean value and have periods of at least 13 days (tides) [6]. From the short mission time, and the required physical models accuracy, this effect is not considered further.
- **Shape:** the spherical and oblate spheroid models will be considered due to one of the termination conditions being related to altitude. Although, the Moon is very spherical and the influence of its flattening is expected to be small [2].
- The **rotation** model of the Moon and Earth are important for the SH gravity field acceleration. Three models are considered: constant axis orientation and rotation rate, synchronous (which is suited for tidally locked bodies such as the Moon), and analytical time varying parameters from Spice.
- **Ephemeris:** Four models will be considered (for all bodies): imported from Spice (most accurate), interpolated from Spice, Keplerian, and constant. As the mission duration is short compared to the period of the Earth's orbit around the Sun, and Moon's orbit around the Earth, it is expected that a highly simplified model will be sufficient.

Throughout this section the Cartesian position and velocity magnitudes will be used as main figures of merit to compare the different settings. The former is commonly used in astrodynamics due to its inherent link to the gravitational acceleration. The velocity is important when considering the need to enter an orbit at the desired altitude³. The altitude is not considered as it is not linked to any acceleration or environment (except shape) model.

¹The mass propagation follows a linear model, hence the mass propagation is always accurate up to rounding errors. The mass will therefore not be considered as main figure of merit in this work.

²Mercury, Venus, Mars, Jupiter, Saturn, Uranus, Neptune

³Which may be a constraint of the optimisation process, eg.

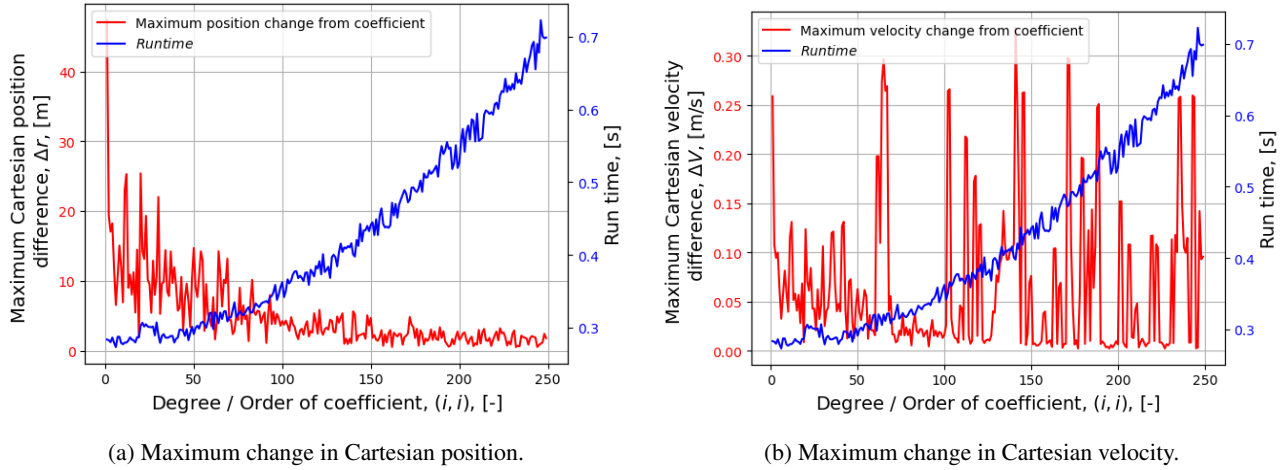


Figure 1: Change in state between propagations with Moon's spherical harmonics gravity field of D/O $(i+1, i+1)$ compared to (i, i) . The CPU runtime associated with the $(i+1, i+1)$ propagation is also displayed.

2.2 Acceleration Models Analysis

The entire acceleration environment is selected in three steps (using TUDAT default settings for the environment). First, the Moon SH acceleration is considered, and the required D/O is selected by comparing the change in state yielded by D/O up to $(i+1, j+1)$ and (i, j) . Second, the change in state arising from the addition of the Earth perturbation is considered with respect to a nominal propagation with only the selected Moon SH and engine thrust as acceleration model⁴, and the need for a SH description of Earth's gravity field is assessed. Third, accelerations due to the Sun (PM and radiation pressure), relativistic corrections, and other planetary bodies are considered with respect to the same nominal case (Moon SH). Except for SH assessments (where the coefficients are added on top of each other), each acceleration is subsequently turned ON and OFF to assess their importance. This permits to decouple the impact of each setting considered. An acceleration is included in the propagation, if it yields a maximum change in state larger than 10% of PROP-1 or -2.

2.2.1 Moon Spherical Harmonics

Fig. 1 shows the change in state between D/O up to $(i+1, i+1)$ and (i, i) ⁵. From both figures, it is clear that the spherical harmonics gravity field is not negligible. However, theoretical expectations indicate that the higher the D/O, the lower the change compared to its direct predecessor, which is clearly not seen here (levelling off in position and semi-random behaviour in velocity). This arises from the initial state of the propagation ($r_0 = 1737.5\text{km}$) starting within the circumscribing sphere of the body ($R_{ref} = 1738\text{km}$). However, the effect itself is small even up to higher orders ($((\frac{R_{ref}}{r_0})^{100} \approx 1.029$ in Eq. (1)) and only lasts for the start of the propagation. The same figure for $r_0 = 1738.5\text{km}$ (outside the circumscribing sphere) is shown in Fig. 2, showing that a very similar behaviour takes place. Therefore, the Moon SH gravity field will still be used even within the circumscribing sphere, without changes to the initial state.

$$U(r, \theta, \phi) = \frac{GM}{r} \sum_{l=0}^{\infty} \sum_{m=0}^l \left(\frac{R_{ref}}{r} \right)^l [\bar{C}_{lm} \cos(m\phi) + \bar{S}_{lm} \sin(m\phi)] P_{lm}(\cos \theta) \quad (1)$$

Based on Fig. 1, it can be concluded that it is not possible to meet both the PROP-4, and the 10% guideline (levelling off at around 2.5m for position accuracy). The present work aims to prepare a propagation setup for an optimisation procedure, where it is especially important to run numerous propagations to find the global optimum. For this reason, a model which is known to be less accurate, but permits to run many more propagations is desired. Therefore, D/O of (75, 75) is selected as its run time is 15% longer than the PM model, while ensuring that adding more terms to the SH description will not result in a maximum Cartesian position change larger than 10m (largest spike past 75x75). Larger D/O could ensure a better accuracy, but at the cost of a rapidly rising run time. In the optimisation process, once a global optimum is found, a more detailed propagation using the thrust settings of the optimum can be performed to verify it with a higher fidelity model. Furthermore, note that the variations in Fig. 1 reflect an oscillation around a 'true' value, as seen in Fig. 3

2.2.2 Earth Spherical Harmonics

A similar analysis for the effect of the Earth spherical harmonics gravity field revealed that only the point-mass gravity term is significant for the perturbation, as seen in Fig. 4. All higher D/O terms were found to be negligible: D/O up to (2, 2) result in a maximum Cartesian position difference of $\mathcal{O}(10^{-5})\text{m}$ with the Earth PM, and even lower for higher D/O.

2.2.3 Other Perturbing Accelerations

Other types of accelerations were considered in Fig. 4, showing that only Earth PM is to be taken into account in the subsequent analysis. The effects of the Sun PM, relativistic corrections, cannonball radiation pressure, and combined third body perturbations of all Solar System planets, are small enough to be discarded. Note that the cannonball radiation

⁴This permits to assess the impact of the perturbing accelerations with respect to a nominal case which is closer to reality.

⁵The number of orders was also kept equal to the number of degrees, as a simplification.

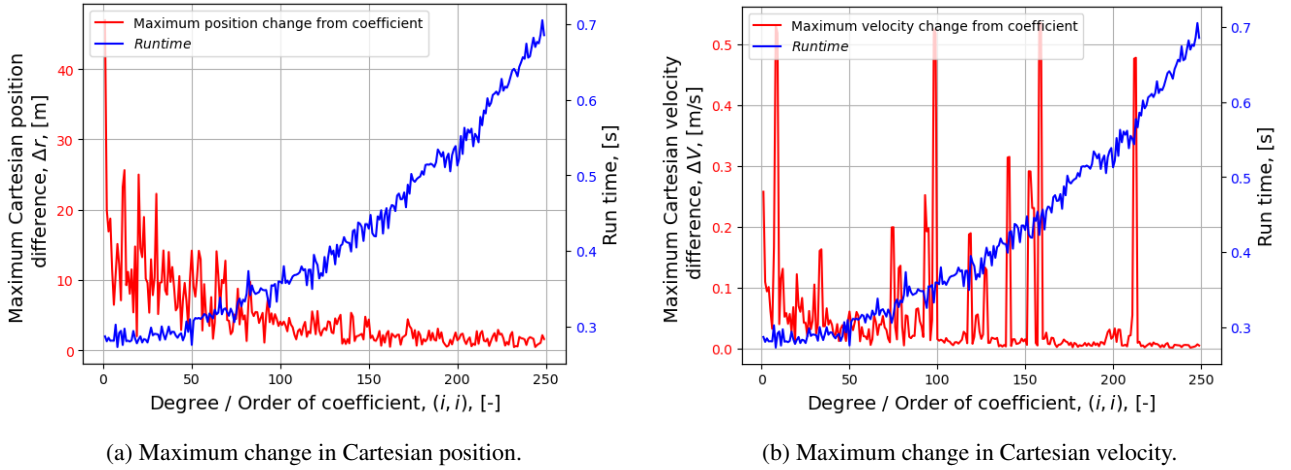


Figure 2: Change in state between propagations with Moon's spherical harmonics gravity field of D/O (i+1, i+1) compared to (i, i), for $r_0 = 1738.5\text{km}$. The CPU runtime associated with the (i+1, i+1) propagation is also displayed.

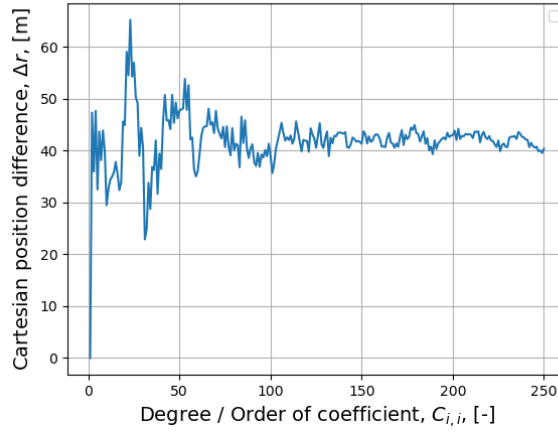


Figure 3: Variation in Cartesian position compared to nominal propagation (Moon PM and engine thrust).

pressure would be zero for this specific start epoch ($t_0 = 0$) with the Moon as an occulting body. Here, no occulting body was defined to assess the magnitude of the perturbing acceleration in case it was present. Furthermore, a coefficient of pressure of $C_p = 1.2$ (from Numerical Astro) and a frontal area of 60m^2 of the Lunar Ascent module were assumed⁶.

2.3 Environment Models Analysis

In the following, simplified environment models are considered with the aim to reduce the propagation CPU time while ensuring an accuracy meeting the physical requirements. This is done in three steps: rotation models of the Moon (Earth is considered a point-mass), ephemerides, and shape models. Throughout this analysis, each variation is compared to a propagation with default TUDAT environment settings and the acceleration environment selected above: Moon SH up to (75, 75), Earth PM, and engine thrust. For the rotation and ephemeris analysis, the default settings are used to assess the accuracy of the models, as they are the most accurate available. Furthermore, this means that the accuracy requirement in Figs. 6 and 5 specifies a maximum change in state which should not be reached by the simplified models to be selected.

2.3.1 Rotation Model

Two simplified rotation models of the Moon were considered: simple from Spice, and the synchronous model. However, the implementation of the latter in TUDAT misses the time-derivative of the rotation matrix, which is necessary for the initial state correction, and therefore will not be considered further. Fig. 5 shows that the simple from spice model comes very close to the accuracy requirement limit within the validity range of the interpolation. However, the full simulation is 100s longer, meaning that the error in the model will likely increase past the accuracy requirement (or come very close). For this reason, the default TUDAT rotation model of the Moon from Spice is selected.

2.3.2 Ephemeris Model

Three simplifications of the default ephemeris model were considered: interpolated data points from Spice (points spaced by 20s and on an interval from $[t_0 - 5\Delta t; t_{max} + 5\Delta t]$ to avoid problems from Runge's phenomenon), Keplerian with initial state from Spice, and constant (Earth and Moon have a fixed Cartesian state in the reference frame, taken from Spice at the start epoch). Note that in the context of optimisation, the interpolation function would be created once for all propagations performed. Following Fig. 6, it appears that the constant model is sufficient to ensure the required

⁶Based on https://history.nasa.gov/alsj/LM04_Lunar_Module_ppLV1-17.pdf [Accessed on 26/05/2023]

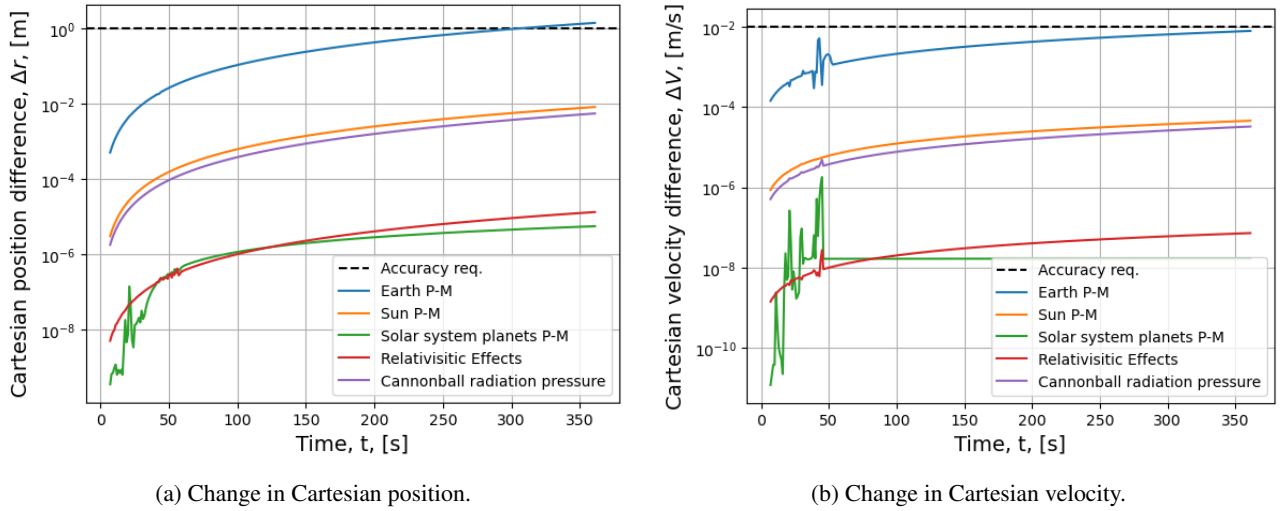


Figure 4: Difference in Cartesian position as a function of time due to different accelerations. Compared to the base acceleration model with the Moon SH (75, 75) and engine thrust.

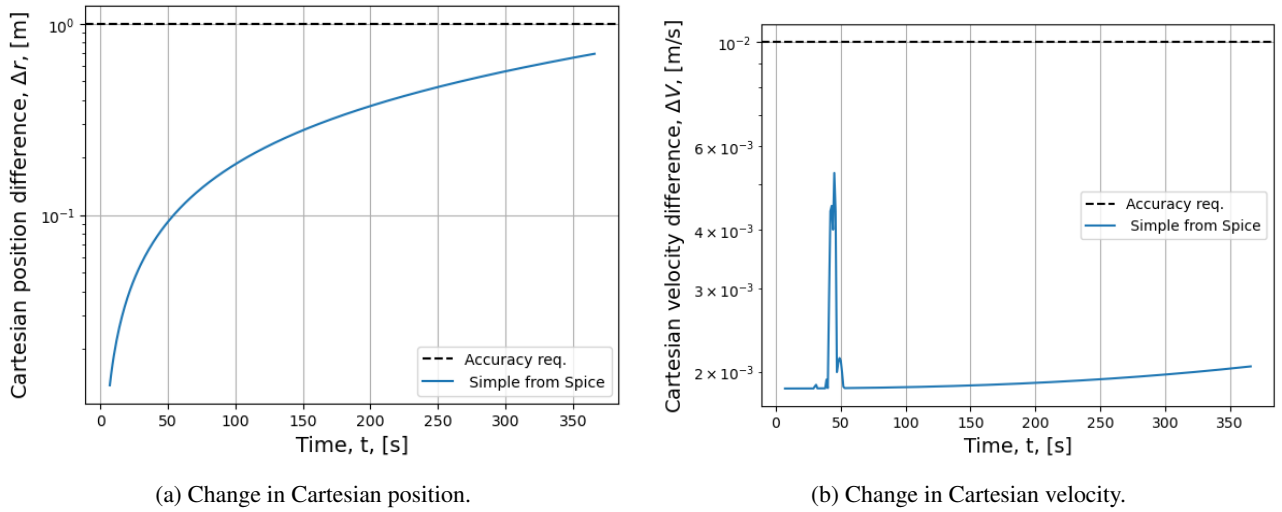


Figure 5: Magnitude of Cartesian position and velocity differences with respect to the same propagation using the Spice rotation model (TUDAT default).

propagation accuracy, while being the least computationally intensive ephemeris model to use. This is due to the mission duration being only $1.9 \times 10^{-2}\%$ of the period of the Moon around the Earth. Furthermore, while the Spice ephemeris are the most accurate available in TUDAT, interpolating those data points results in interpolation errors, which are the driving cause for the inaccuracies seen in Fig. 6. The Keplerian ephemeris provides the best fit (difference goes to rounding error) to the nominal (Spice) propagation as the Keplerian elements of the Moon's orbit around the Earth do not change much over 450s. However, this accuracy is not necessary, and the simplest model (constant ephemeris) is selected.

2.3.3 Shape Model

Both the spherical (TUDAT default) and oblate spheroid⁷ models of the Moon were considered. However, the propagation fails as the vehicle is inside the Moon. Changing the initial position to be at 100m altitude above the oblate spheroid, the propagation shows that the altitude is only changed by 0.3m. This is below the 10% guideline on the position, and no effect on the velocity result. Furthermore, changing from one model or the other does not influence either the Cartesian state or the acceleration models computation. Therefore, a spherical model is selected for simplicity.

2.4 Recommendations on Acceleration and Environment Models Selection

The acceleration model was selected based on the guideline that all accelerations which single-handedly change the state by at least 10% of the physical requirement specification, are to be included. However, this guideline could not be met for the selection of the degree and order of the spherical harmonic gravity field of the Moon, due to the proximity of the vehicle with the circumscribing sphere limit, and high computational load associated with high D/O representations. Spherical harmonics of the Moon up to D/O (75, 75) were selected as a trade-off between PROP-1,2 and PROP-4 (16% longer runtime but only roughly 10m and 0.3m/s accuracy). Following, the proximity of the Earth to the Moon results in a relatively large perturbing acceleration due to its PM gravity field, and cannot be neglected. The short duration of the mission results in a smaller effect of other perturbing accelerations, such as the spherical harmonics of the Earth, the

⁷With flattening coefficient $f = 0.0012$ and radius $R = 1738.1\text{km}$.

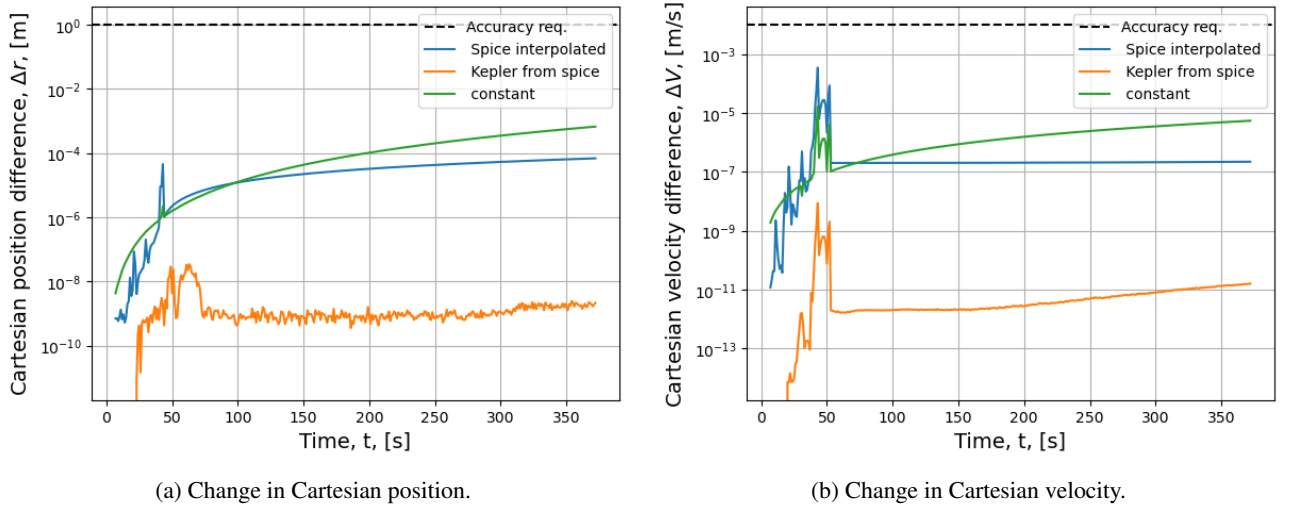


Figure 6: Magnitude of Cartesian position and velocity differences with respect to the same propagation using the Spice ephemeris (TUDAT default).

Sun gravity field and cannonball radiation pressure, the third body accelerations of the solar system planets, as well as relativistic corrections. However, for higher accuracy propagations (such as the final check after finding an optimum in the optimisation), the next two most important perturbing accelerations are the Sun PM and cannonball radiation pressure. Having selected the acceleration models, the environment models were considered to simplify the propagation setup and reduce the computational load. Due to the very high importance of the Moon SH gravity field in the acceleration model, a high accuracy model of the Moon rotation is necessary. For this purpose the rotation model from Spice is used (highest fidelity model available in TUDAT). Although other more accurate rotation models of the Moon exist, this one is considered to be accurate enough due to the very short duration of the mission. The ephemeris model of the Earth (and Moon) could be simplified to a constant model, where their state is fixed with respect to each other. This is also a direct result of the mission duration being about 0.019% of the Moon’s orbital period, meaning that its motion is negligible. Finally, the shape models were found to have a negligible effect on the propagation (termination condition shifted by 0.3m only). Therefore, the simplest model (spherical shape) was selected.

3 Uncertainty Analysis

In this section, an uncertainty analysis on the acceleration and environment models setup above is performed.

3.1 Major Uncertainties

Uncertainties in the propagation setup above can arise from either the parameters used in the models, or from the accuracy of the models themselves (how well does the model represent reality). The major sources of uncertainties in the propagation setup arise from the following:

1. **Moon gravity field:** a SH representation of the gravity field of the Moon is used, meaning that uncertainties in both the body’s gravitational parameter (μ_M), and the \bar{C}_{lm} and \bar{S}_{lm} coefficients, could have a large impact on the trajectory. Specifically, it was seen in Fig. 1 that adding SH coefficients up to (2, 2), causes a maximum deviation of about 50m with respect to the point mass gravity field trajectory. This effect is primarily due to $\bar{C}_{2,0} = J_2$ in the SH field.
2. **Earth gravity field:** a PM gravity field description of the Earth is used in the model, meaning that only uncertainties in its gravitational parameter (μ_E) have an effect on the propagation. This effect is likely small, however, due to the very small relative uncertainty in this parameter (see Tab. 2).
3. **Engine thrust:** uncertainties in the engine thrust acceleration (magnitude or orientation) can have a large effect on the resulting trajectory, as it is the primary acceleration throughout the propagation. However, the thrust model is dictated by the propagation input parameters which will be optimised in subsequent work. Analysis of the uncertainties surrounding the thrust model will likely be conducted to verify the sensitivity of the optimum found after the optimisation process (to assess whether small changes in inputs result in large performance changes). For this reason, this model was not considered further for the uncertainty analysis.
4. **Rotation model:** a major part of the acceleration model is the SH gravity field of the Moon, which depends on the orientation of the body at a particular time. As can be seen in Fig. 5, despite the very short mission time, the model cannot be simplified to a constant rotation rate and pole orientation. This shows that the effect of the rotation model on the propagation is important, and its uncertainty could have a large impact. However, the Spice rotation model parameters cannot be varied, meaning that no uncertainty analysis can be performed.

Furthermore, it was shown in Fig. 4 that the relativistic correction terms have a negligible effect on the propagation. As a result, it can be concluded that the uncertainty in the state derivative formulation arising from the gravitational accelerations is negligible, as those corrections aim to better match Newton’s gravitational model for first order effects of General Relativity (which is a higher accuracy model). Following, the ephemeris description was highly simplified in the previous section (constant model), and the majority of the uncertainty was quantified in Fig. 6a, showing that it is low

Table 2: Major uncertainties in the acceleration models [6, 7]. Note that the exact values used here may not be the ones part of TUDAT, but the uncertainties can reasonably be assumed to be similar.

Parameter	Value and uncertainty
μ_E	$3.986004415e14 \pm 8e5 \text{ m}^3/\text{s}^2$
μ_M	$4902.80031 \pm 0.00044 \text{ m}^3/\text{s}^2$
\bar{J}_2	$9.0880835e-5 \pm 1.4e-9$
$\bar{C}_{2,2}$	$3.4673798e-5 \pm 1.7e-9$

enough for the purpose of this work. Small variations of the state of the Earth and Moon with respect to each other will always result in a smaller uncertainty than the simplification, due to the low uncertainty in the states provided by Spice at the start epoch. Additionally, the shape model was shown to have no effect on the propagation itself and therefore its uncertainties can be discarded.

As a result, the main uncertainties (which can be analysed) in the model arise from the gravitational parameters of the Moon and Earth. μ_E , μ_M , \bar{J}_2 , and $\bar{C}_{2,2}$, are the parameters with uncertainties which can potentially affect the propagation the most. In order to analyse different types of uncertainties, \bar{J}_2 and μ_M will be considered in this section⁸.

3.2 Propagation Error due to Uncertainty

A Monte Carlo simulation of the propagation was set up by assuming that the uncertainties shown in Tab. 2 follow a normal distribution with the form $\mu \pm \sigma$ (μ the mean value and σ the standard deviation). For each case, a random deviation from the mean is computed using the *random.gauss* method, which uses a Box-Muller Transform to generate a sequence of pseudo-random numbers following the normal distribution (μ , σ). Seed 42 was used to produce the final results⁹. Each case was compared to the nominal (no parameter change) propagation. Furthermore, the Cartesian position, and Cartesian velocity will be used as figures of merit for the analysis. Note that the RKF4(5) integrator was used with tolerances of 1e-10 to ensure position and velocity accuracy of 2e-4m and 2e-7m/s respectively, as the deviations from the nominal case were found to be small.

First considering the analysis in \bar{J}_2 , Figs 7 and 8 show the distribution of the deviations in the parameter for 3000 and 1500 data points respectively, showing that the distributions are very similar (and similar conclusions would be drawn). This variation in \bar{J}_2 causes a variation in the final Cartesian position and velocity magnitudes as seen in Fig. 9. It is directly clear that the effect of the uncertainty in \bar{J}_2 is very small (order of [mm] and [$\mu\text{m/s}$]). Following, it is seen from Fig. 10 that the difference with respect to the nominal grows linearly in time for the Δv and close to parabolically for Δr . This means that the difference compounds with time and may become more significant if the mission was longer. Furthermore, Fig. 12 gives the percentage of the propagations which are within 1mm (position) and 10 $\mu\text{m/s}$ (velocity) with respect to the value obtained using the sensitivity matrix S (Eq. (2), parameter p). Figs. 11 and 12 demonstrate that the behaviour is linear throughout the entire uncertainty range, as expected (small uncertainty and short mission duration).

$$\Delta \mathbf{x}_E = S(t_E) \Delta \mathbf{p} \quad (2)$$

The effect of the uncertainty in μ_M has a very similar behaviour to the one of \bar{J}_2 , although it is about 20 times larger. Figs. 13 and 14 shows that 3000 samples is enough to draw meaningful conclusions from the analysis, and the distributions in Fig. 15 show an effect on the position and velocity of the order of 30-40mm and 0.15-0.2mm/s at most, respectively. The effect of the uncertainty is then negligible. The same conclusions as drawn for \bar{J}_2 is applicable for Fig. 16, showing that the effect of a change in μ_M compounds over time. Finally, Figs. 17 and 18 show that the behaviour is again very linear, but less than the effect of \bar{J}_2 (as expected as the parameter itself has a larger impact on the trajectory).

⁸Note that μ_E was first considered, showing that the effect of its uncertainty is well below integration errors.

⁹[https://en.wikipedia.org/wiki/The_Hitchhiker%27s_Guide_to_the_Galaxy_\(novel\)](https://en.wikipedia.org/wiki/The_Hitchhiker%27s_Guide_to_the_Galaxy_(novel)) [Accessed on 31/05/2023]

3.2.1 Plots of Monte Carlo simulation of \bar{J}_2

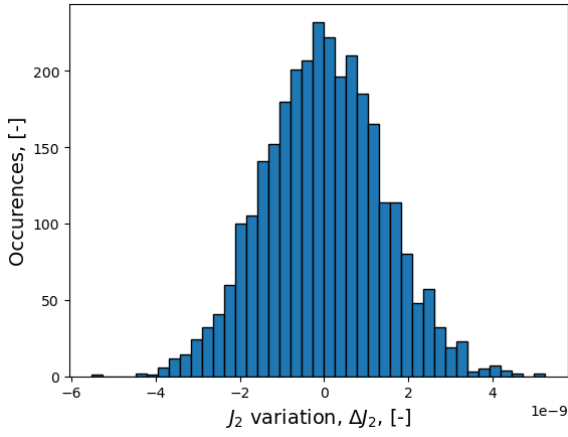


Figure 7: Deviations from the nominal \bar{J}_2 value, based on a total of 3000 samples.

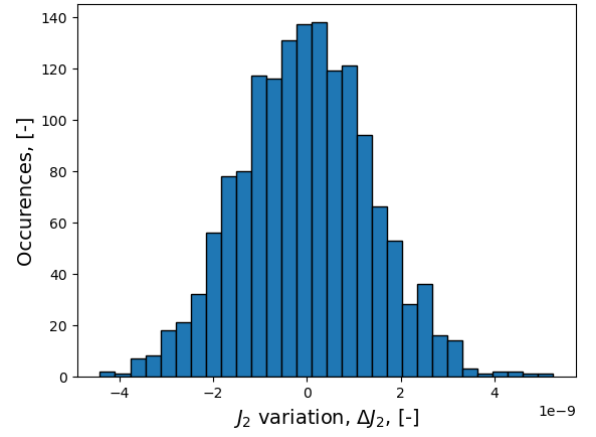
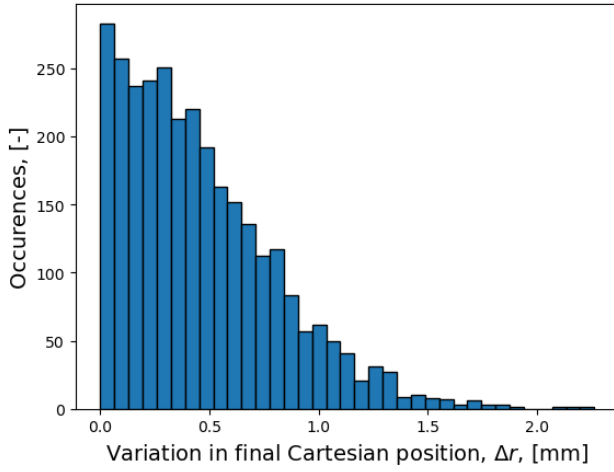
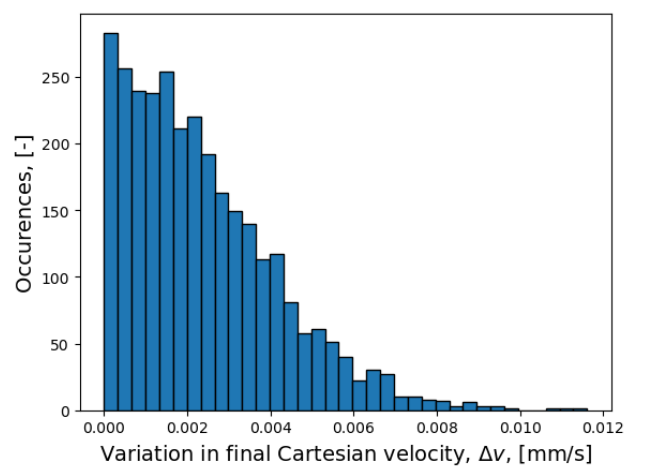


Figure 8: Deviations from the nominal \bar{J}_2 value, based on a total of 1500 samples.

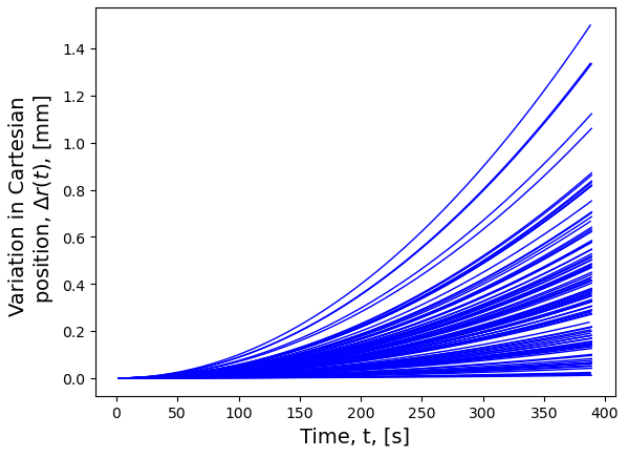


(a) Final change in Cartesian position.

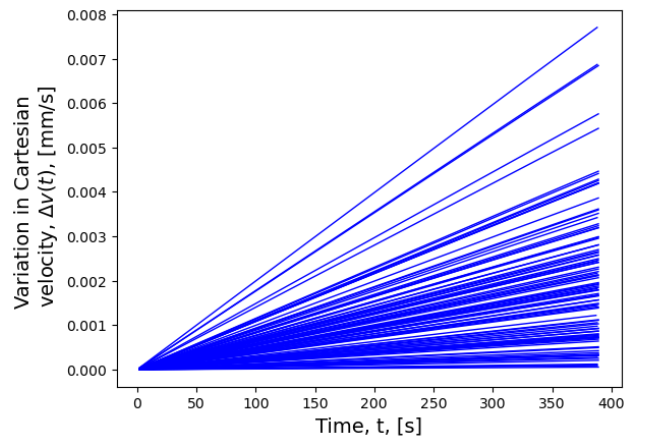


(b) Final change in Cartesian velocity.

Figure 9: Distributions of the Cartesian position and velocity at the end of the propagation due to variations in \bar{J}_2 . Data generated using 3000 samples.



(a) Cartesian position difference to the nominal case.



(b) Cartesian velocity difference to the nominal case.

Figure 10: Cartesian state differences with respect to the nominal case (no deviations in \bar{J}_2), as a function of time. Generated with 100 propagations.

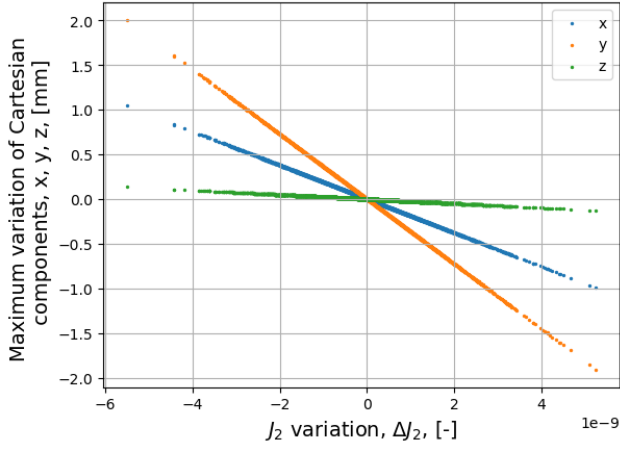


Figure 11: Difference of Cartesian components with respect to the nominal case (no deviations in J_2), as a function of the deviation.

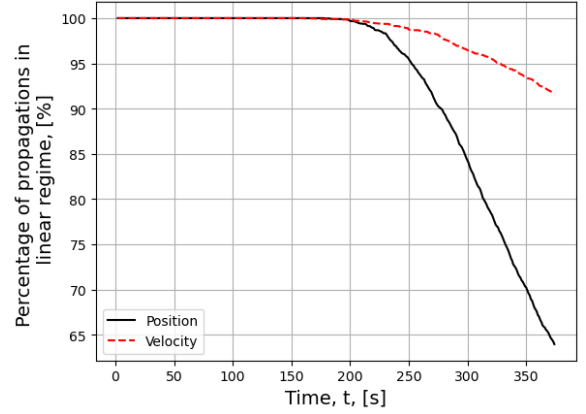


Figure 12: Caption

3.2.2 Plots of Monte Carlo simulation of μ_M

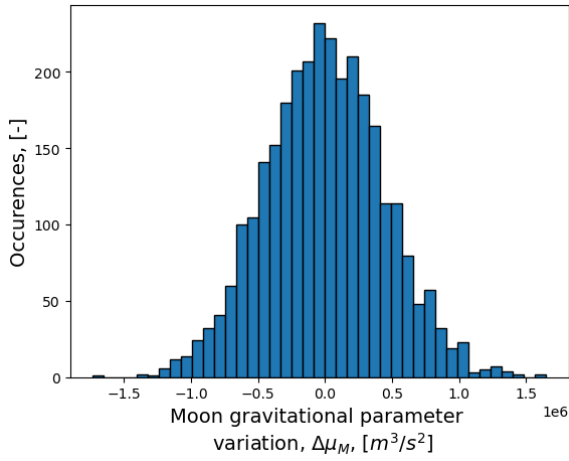


Figure 13: Deviations from the nominal μ_M value, based on a total of 3000 samples.

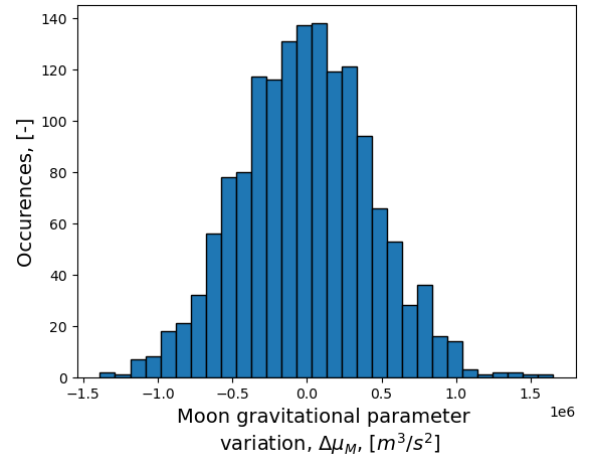
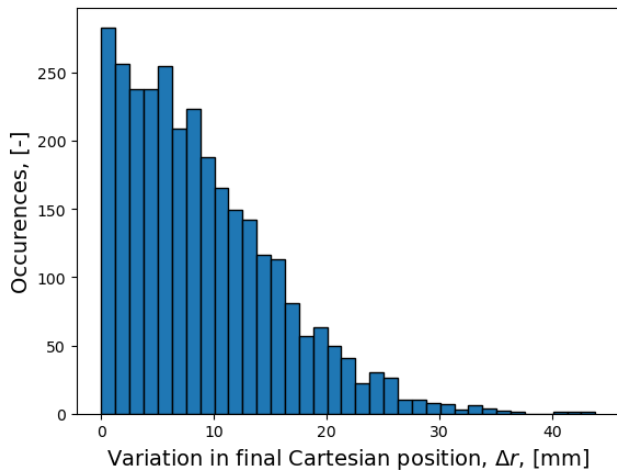
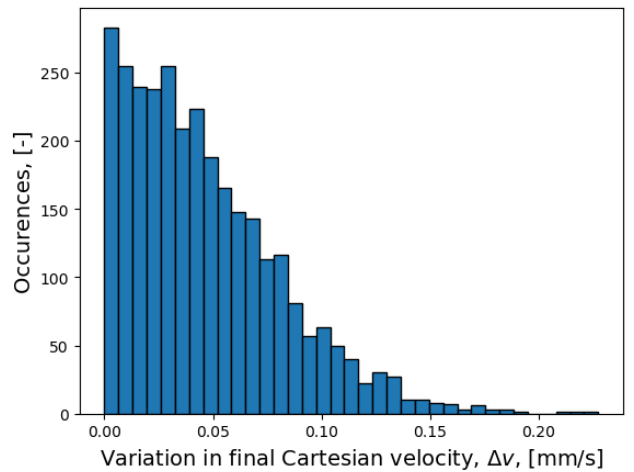


Figure 14: Deviations from the nominal μ_M value, based on a total of 1500 samples.

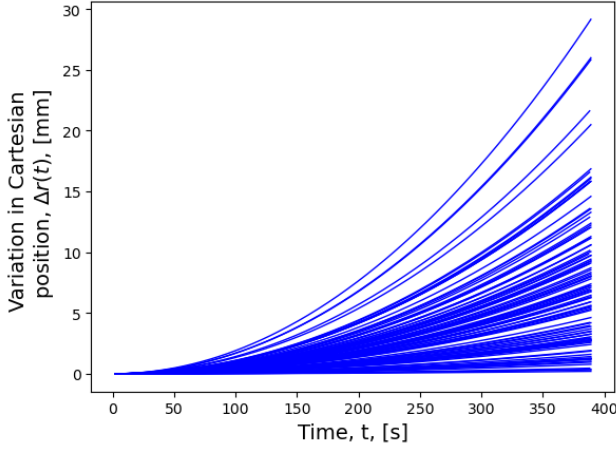


(a) Final change in Cartesian position.

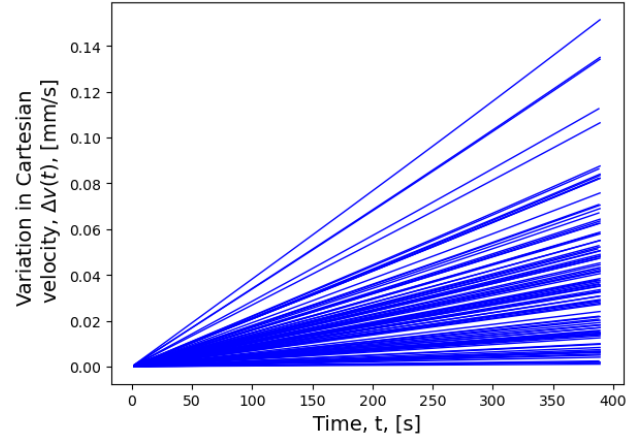


(b) Final change in Cartesian velocity.

Figure 15: Distributions of the Cartesian position and velocity at the end of the propagation due to variations in μ_M . Data generated using 3000 samples.



(a) Cartesian position difference to the nominal case.



(b) Cartesian velocity difference to the nominal case.

Figure 16: Cartesian state differences with respect to the nominal case (no deviations in μ_M), as a function of time. Generated with 250 propagations.

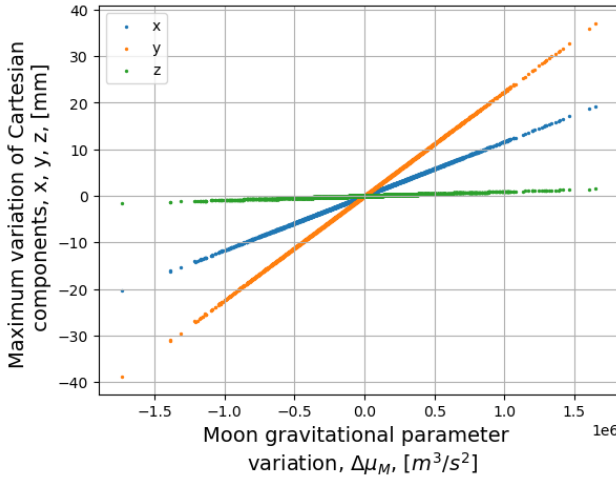


Figure 17: Difference of Cartesian components with respect to the nominal case (no deviations in μ_M), as a function of the deviation.

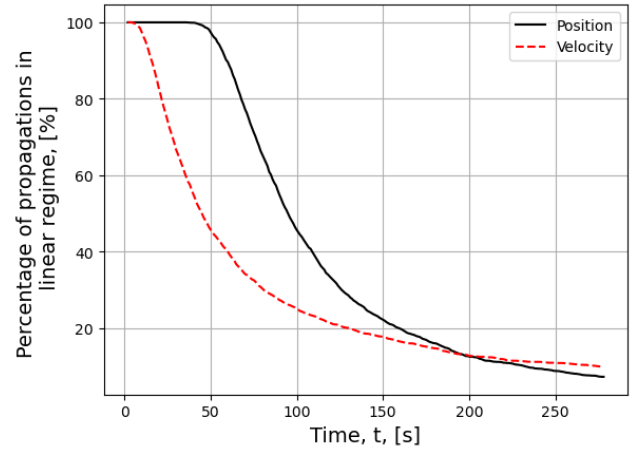


Figure 18: Caption

3.3 Mitigation of Uncertainties

It was seen above that the major uncertainties in the model, only cause very small variations in the trajectory (order of centimetres at most). However, larger uncertainties arising from the simplification of the acceleration environment were quantified in Section 1. Most importantly, it was shown that the SH series had to be truncated at D/O (75, 75), from a trade-off between accuracy and CPU time. This resulted in an uncertainty in Cartesian position and velocity of the order of 10m and 0.3m/s (respectively) at most, meaning that PROP-1,2 cannot be met for this particular part of the acceleration model. If the trajectory produced by the optimisation was to be used without further iterations, the use of a guidance algorithm throughout the trajectory could reduce the uncertainties in the final position and velocity using corrections throughout the ascent. However, in practice the optimal parameters found would be used in a very high accuracy simulation (best available integrator, acceleration model and environment model) to verify its performance in a single run. The need for guidance would then be reduced significantly. Similarly, uncertainties in the physical thrust model (alignment, magnitude) could be tackled through the use of a guidance algorithm.

4 Final Recommendation

4.1 Model Settings

The following list of settings is recommended for the optimisation process:

- **Integrator:** RKF4(5) variable step with (absolute and relative) tolerances of $1e-7$.
- **Propagator:** Cowell.
- **Acceleration model:** Moon spherical harmonics up to D/O (75, 75), Earth point-mass, and engine thrust.
- **Environment model:** constant ephemeris, Spice rotation model (TUDAT default), and spherical shape model.

This combination of settings provides a reliable and robust (with respect to the input thrust parameters) description of the physical problem. A single propagation runs within about 0.27s (392 function evaluations, without Δt_{max}); the

integrator-propagator combination ensures numerical errors in position and velocity of maximum $5.26\text{e-}2\text{m}$ and $6.95\text{e-}05\text{m/s}$ respectively; all accelerations having an effect on the propagation state larger than 10% of PROP-1,2 were taken into account; and environment models were simplified as much as possible to reduce the computational load per propagation. However, the guideline of 10% of the physical requirements could not be satisfied for the spherical harmonics description of the Moon, where truncated terms can cause variations in the propagation state violating the guideline. This truncation was necessary, however, as a trade-off between propagation CPU time and accuracy. Furthermore, the integrator-propagator choice from Veithen [1] was not revisited as it satisfies the numerical accuracy requirements, and the Cowell propagator is very robust to the thrust input parameters¹⁰.

4.2 Optimisation Formulation

The problem tackle in the two first assignments considers the trajectory in a near-equatorial plane, and the formulation does not permit to model a 3D orbit. Furthermore, the trajectory is discretised in 5 nodes, where the thrust angle can change, but not the thrust magnitude. Those simplifications are necessary to avoid a too large design space, as the time to find an optimum scales with the dimension of the problem. However, the use of a constant thrust magnitude is very constraining, hence the author suggests using it as a design variable at each node. Alternatively, the distance between the thrust nodes could be variable from one to another (but not both a variation in thrust magnitude, and in node placement, as that would result in a too complex problem). The following optimisation formulation is suggested:

1. **Decision variables:** fixed Δt between the nodes, variable thrust T , variable thrust angle θ : $[T_1, T_2, T_3, T_4, T_5, \Delta t, \theta_1, \theta_2, \theta_3, \theta_4, \theta_5]$; or variable Δt , constant thrust, and variable thrust angles: $[T, \Delta t_1, \Delta t_2, \Delta t_3, \Delta t_4, \theta_1, \theta_2, \theta_3, \theta_4, \theta_5]$.
2. **Constraints:**
 - Orbital altitude: $\|\mathbf{r}_{min}\| \leq \|\mathbf{r}\| \leq \|\mathbf{r}_{max}\|$. The module shall be inserted in the right orbit.
 - Orbit insertion, within an acceptable range: $x_{i,min} \leq x_{i,f} \leq x_{i,max}$, with i refers to a component of the Cartesian velocity vector. Note that the values of minimum and maximum of each component should be position dependent (at the right orbital altitude) to ensure freedom in where the orbit insertion takes place (in space). Furthermore, the constraints should be small enough for a guidance algorithm to be able to correct the deviations.
 - Maximum mechanical load (due to structure or payload): $\frac{T}{Mg} \leq a_{max}$.
 - Maximum and minimum thrust (due to the engine specification: $T_{min} \leq T \leq T_{max}$. And fixed engine specifications: $I_{sp} = I_{sp, specification}$
 - Final mass is the dry mass: $M_{dry} \leq M$.
 - No crash with the surface: $0 \leq h$, altitude larger than zero.
 - Maximum angular rate of the thrust vector: $\dot{\theta} \leq \dot{\theta}_{max}$. The Attitude Determination and Control System of the vehicle should be able to keep up with the thrust orientation (assuming no gimbal on the thrust nozzle).
 - Maximum mission time: $t \leq t_{max}$.
3. **Objectives:** minimize the propellant mass consumption (mostly equivalent to minimising ΔV , but the mass is a state variable, meaning that it is easier to formulate its optimisation): minimise $M_0 - M_{dry}$.

¹⁰Which is desired for optimisation as a wide range of input variables will be considered, and the numerical accuracy should stay stable

References

- [1] L. Veithen, “Lunar ascent trajectory propagation and optimisation - integrator and propagator selection,” Delft University of Technology, Tech. Rep., 2023.
- [2] M. Boere, “Optimization of descent trajectories for lunar base settlement,” 2010.
- [3] R. B. Roncoli, *Lunar constants and models document*. Jet Propulsion Laboratory, 2005.
- [4] A. Wilhite, R. Tolson, M. Mazur, and J. Wagner, “Lunar module descent mission design,” in *AIAA/AAS Astrodynamics Specialist Conference and Exhibit*, 2008, p. 6939.
- [5] L. Ma, W. Chen, Z. Song, and Z. Shao, “A unified trajectory optimization framework for lunar ascent,” *Advances in Engineering Software*, vol. 94, pp. 32–45, 2016, ISSN: 0965-9978. DOI: <https://doi.org/10.1016/j.advengsoft.2016.01.002>. [Online]. Available: <https://www.sciencedirect.com/science/article/pii/S0965997816300102>.
- [6] A. S. Konopliv *et al.*, “The jpl lunar gravity field to spherical harmonic degree 660 from the grail primary mission,” *Journal of Geophysical Research: Planets*, vol. 118, no. 7, pp. 1415–1434, 2013. DOI: <https://doi.org/10.1002/jgre.20097>. eprint: <https://agupubs.onlinelibrary.wiley.com/doi/pdf/10.1002/jgre.20097>. [Online]. Available: <https://agupubs.onlinelibrary.wiley.com/doi/abs/10.1002/jgre.20097>.
- [7] I. D. I. W. Group. “Astronomical constants : Current best estimates (cbes).” (2012), [Online]. Available: https://iau-a3.gitlab.io/NSFA/NSFA_cbe.html#GME2009.